Advances in Concrete Construction, *Vol. 7, No. 1 (2019) 39-50*
DOI: https://doi.org/10.12989/acc.2019.7.1.039

Comprehensive experimental investigation on mechanical behavior for types of reinforced concrete Haunched beam

Hasan M. Albegmprli*[1], M. Eren Gülşan[2a] and Abdulkadir Cevik[2b]

[1]*Engineering Technical College, Building and Construction Engineering Department, Northern Technical University, Mosul, Iraq*
[2]*Civil Engineering Department, Gaziantep University, University Avenue - Central Campus, Gaziantep, Turkey*

(Received July 20, 2018, Revised January 14, 2019, Accepted January 15, 2019)

Abstract. This study presents a comprehensive experimental investigation on mostly encountered types of Reinforced Concrete Haunched Beams (RCHBs) where three modes of RCHBs investigated; the diversity of studied beams makes it a pioneer in this topic. The experimental study consists of twenty RCHBs and four prismatic beams. Effects of important parameters including beam type, the inclination angle, flexure and compressive reinforcement, shear reinforcement on mechanical behavior and failure mode of each mode of RCHBs were examined in detail. Furthermore crack propagation at certain load levels were inspected and visualized for each RCHB mode. The results confirm that RCHBs have different behavior in shear as compared to the prismatic beams. At the same time, different mechanical behavior was observed between the modes of RCHBs. Therefore, RCHBs were classified into three modes according to the inclination shape and mode of failure (Modes A, B and C). However, it was observed that there is no significant difference between RCHBs and prismatic beams regarding flexural behavior. Moreover, a new and unified formula was proposed to predict the critical effective depth of all modes of RCHBs that is very useful to predict the critical section for failure.

Keywords: Haunched beams; load capacity; load-deflection curve; failure mode; crack propagation

1. Introduction

Reinforced concrete haunched beams (RCHBs) have been extensively preferred in industrial buildings, bridges, structural portal frames and framed buildings due to its several advantages (Hou *et al*. 2015). Weight of structure can be reduced and larger spans can be achieved by the use of RCHBs instead of prismatic beam without a clear deterioration in loading capacity (Naik and Manjunath 2017). Despite of these advantages, very few studies have been investigated on the behavior of RCHBs so far. Therefore, the experimental and theoretical background about mechanical behavior of RCHBs should be improved. However, it should be noted that since effective depth of RCHBs is variable along the length of the beams, structural analysis and mechanical behavior of them differ from the analysis and behavior of prismatic beams. The first experimental study was carried out by (Debaiky and Elniema 1982) to investigate the shear behavior of RCHBs. The authors proved that the nominal shear contribution of the concrete and the longitudinal reinforcement were influenced by the haunch's inclination.

El-Niema (1988) published another study investigated of T-section RCHBs. The results did not show substantial difference in the mechanical behavior and strength capacity as compared to the rectangular section RCHBs. (Stefanou 1983) conducted an experimental study of shear resistance on reinforced concrete beams with non-prismatic sections for two types of RCHBs. (Macleod and Houmsi 1994) published a study about shear strength of RCHBs. The main conclusion for both studies was decreasing the volume of concrete in the beam due to increasing slope angle improves the shear strength capacity and the failure to be more ductile.

Tena *et al*. (2008) have tested eight prototypes of RCHBs. The study investigated only one type of RCHBs with different inclination angle. The authors concluded that the RCHBs have more ductility than the prismatic beams and the shear strength was increased in the RCHBs. (Nghiep 2011) studied the shear design of RCHBs without shear reinforcement where all of the RCHBs had inclined at compression zone. The main outcome was that inclination had a high influence on the shear capacity. Zanuy *et al*. (2015) presented results of fatigue tests on the RCHBs without stirrups. Two types of failure modes have been obtained due to fatigue of the reinforcement or shear fatigue. The study concluded that the RCHBs without shear reinforcement are able to suffer fatigue. Hans *et al*. (2013) tested prototype simply supported RCHBs under cyclic loading were all the beams have the same inclination case, the authors observed that haunched beams have a different cyclic shear behavior with respect to prismatic beams, having higher deformation and energy dissipation capacities.

Chenwei *et al*. (2015) studied the shear failure

*Corresponding author, Ph.D.
E-mail: albegmprli@ntu.edu.iq
[a]Assistant Professor
E-mail: gulsan@gantep.edu.tr
[b]Professor
E-mail: akcevik@gantep.edu.tr

 ISSN: 2287-5301 (Print), 2287-531X (Online)

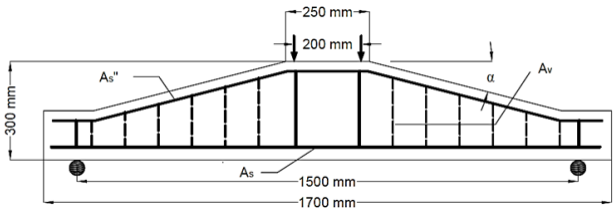

Fig. 1 Details of the beams for Mode A

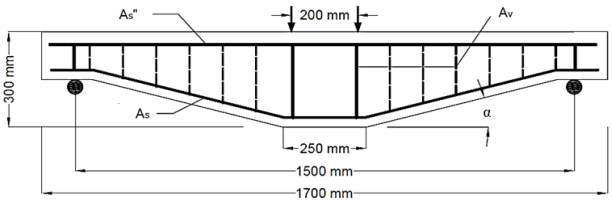

Fig. 2 Details of the beams for Mode B

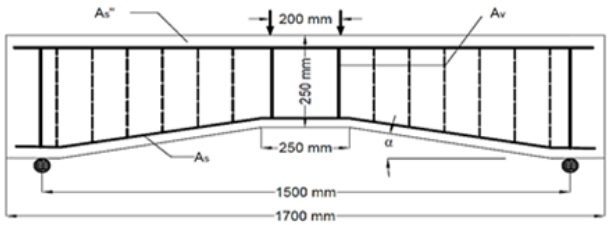

Fig. 3 Details of the beams for Mode C

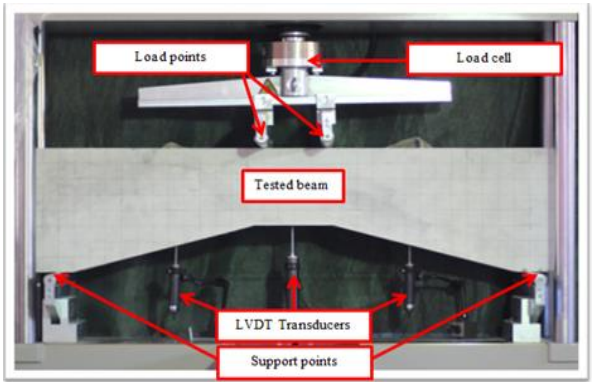

Fig. 4 Testing the specimen

mechanism of RCHBs. All beams were inclined from upper face and the thickness increased in the support. The results demonstrated that the bent tensile rebar has a negative contribution to the shear capacity. Albegmprli *et al*. (2015) carried out a theoretical study about the ultimate shear capacity of RCHBs. The study performed stochastic and reliability analyses based on nonlinear finite element analysis. The authors evaluated the influence of material properties and geometry parameters as uncertain values on the mechanical behavior of RCHBs. Gulsan *et al*. (2018) studied finite element modeling and proposed a new design code formulation to improve the shear design equation of ACI-318 to be more suitable to design the RCHBs, Eq. (4).

Although there are several experimental studies regarding mechanical behavior of several modes of RCHBs, there is no any study which investigated different modes of these beams simultaneously. Moreover, the best choice should be investigated by analysis of superiority of several RCHBs modes to each other regarding load capacity, crack pattern, post peak behavior, failure mode etc. The current study aims to close this gap in literature. The main objectives of this study are investigation of the mechanical behavior of RCHBs as compared to prismatic beams, influence of the differences between the modes of RCHBs regarding to mechanical behavior, identification of crack propagation and failure shape of all modes of RCHBs and research on contribution of the shear reinforcement and inclined longitudinal reinforcement to the behavior of RCHBs.

2. Experimental program

2.1 The specimens

The experimental program includes 24 specimens belonging to three modes depending on the beam shape. Four of beams are prismatic and the others have variable depths. The RCHBs were classified into three modes A, B&C regarding to geometry of the beam. The geometries of the tested beams are selected to have more simulation of practical reality, the modes as follows:

- Mode A refers to RCHBs inclined at the compression face. In this mode, the depth of the beams decreases in the support.
- Mode B refers to RCHBs inclined at the tension face, the depth of the beams decreases toward the support and the sign of the inclination angle is assumed to be positive.
- Mode C refers to RCHBs inclined at the tension face, the depth of the beam increases toward the support and the sign of the angle is assumed to be negative.

Total length, width and span length of all beams were fixed 1700 mm, 150 mm and 1500 mm, respectively. The effective depth of the beams at the mid-span was taken 260 mm for modes A&B, and 210 mm for mode C to achieve the target shear span ratio condition (a/d>2.5). The experimental program consisted, nine beams in Mode A, seven beams in Mode B and eight beams in Mode C, the details of RCHBs cases are detailed in Figs. 1, 2 and 3. The geometries of all the beams are summarized in Table 1.

2.3 Testing procedure

All of the beams were tested using a 500 kN capacity displacement controlled servo hydraulic flexural testing machine. The load application was controlled using an advanced hydraulic system. All of the beams were tested according to four point bending test as shown in Fig. 4. The span length is 1500 mm and the spacing between two loading points is 200 mm. The beams were supported on two steel rollers, one of them is allowed to rotate and other is not permitted to prevent the axial load on the supports. The loading tests were carried out by displacement controlled mode; the displacement was increased by 0.2 mm at each loading step controlled by a displacement

Table 1 Geometries of the specimens

Beam	Mode	$\alpha°$ [1]	h_o [2] (mm)	h_s [3] (mm)	A_s [4] (mm^2)	A_s" [5] (mm^2)	ρ_v % [6]
A0-0	-	0	300	300	603 (3Ø 16)	100 (2Ø 8)	-
A0-2	-	0	300	300	603 (3Ø 16)	100 (2Ø 8)	0.67
A1-0	A	4.97	300	250	603 (3Ø 16)	100 (2Ø 8)	-
A2-0	A	9.87	300	200	603 (3Ø 16)	100 (2Ø 8)	-
A2-1	A	9.87	300	200	603 (3Ø 16)	308 (2Ø 14)	-
A2-2	A	9.87	300	200	603 (3Ø 16)	100 (2Ø 8)	0.67
A3-0	A	14.62	300	150	603 (3Ø 16)	100 (2Ø 8)	-
A3-1	A	14.62	300	150	603 (3Ø 16)	308 (2Ø 14)	-
A3-2	A	14.62	300	150	603 (3Ø 16)	100 (2Ø 8)	0.67
B0-0	-	0	300	300	603 (3Ø 16)	100 (2Ø 8)	-
B1-0	B	4.97	300	250	603 (3Ø 16)	100 (2Ø 8)	-
B2-0	B	9.87	300	200	603 (3Ø 16)	100 (2Ø 8)	-
B2-1	B	9.87	300	200	402 (2Ø 16)	100 (2Ø 8)	-
B3-0	B	14.62	300	150	603 (3Ø 16)	100 (2Ø 8)	-
B3-1	B	14.62	300	150	402 (2Ø 16)	100 (2Ø 8)	-
B3-2	B	14.62	300	150	603 (3Ø 16)	100 (2Ø 8)	0.67
C0-0	-	0	250	250	603 (3Ø 16)	100 (2Ø 8)	-
C1-0	C	-4.97	250	300	603 (3Ø 16)	100 (2Ø 8)	-
C2-0	C	-9.87	250	350	603 (3Ø 16)	100 (2Ø 8)	-
C2-1	C	-9.87	250	350	402 (2Ø 16)	100 (2Ø 8)	-
C2-2	C	-9.87	250	350	603 (3Ø 16)	100 (2Ø 8)	0.67
C3-0	C	-14.62	250	400	603 (3Ø 16)	100 (2Ø 8)	-
C3-1	C	-14.62	250	400	402 (2Ø 16)	100 (2Ø 8)	-
C3-2	C	-14.62	250	400	603 (3Ø 16)	100 (2Ø 8)	0.67

[1] Inclination angle; [2] Depth at mid-span; [3] Depth at supports; [4] Flexural reinforcement;
[5] Compression reinforcement; [6] Shear reinforcement percentages (Ø 8@100 mm).

Table 2 Concrete mix proportions

Material	Gravel	Sand	Cement	Fly Ash	Silica Fume	Water	Visco-Crete
kg/m^3	680	1100	250	215	35	150	5

sensor until beam failure. The recorded values in each step of loading consist of load, displacement and crack propagation. Test configuration of the beams is shown in Fig. 4. Following instruments were used for measuring and monitoring during loading tests:

- A load cell to record the load value.
- Three linear variable displacement transducers (LVDTs) to measure deflections in middle of the beam and in middle of the span that extends between the supports and the loading points.
- A high resolution camera for monitoring the beam and following the crack propagation.
- A high magnification camera to detect formation of cracks, especially for first cracks.

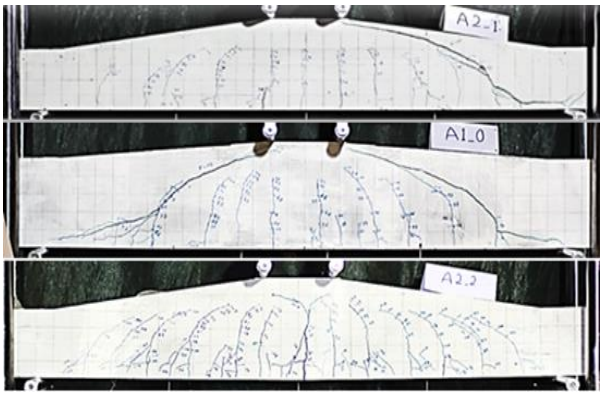

Fig. 5 Failure modes

3. Testing results

3.1 Load capacity and failure modes

All of beams were tested in displacement controlled mode until failure. As expected, the beams which were without shear reinforcement failed in shear. In general, the diagonal shear crack showed up suddenly between the support and the loading point. The shear crack occurred on either one side or both sides of the beam. However, the beams that were reinforced with stirrups in addition to main reinforcement failed in flexural mode; see Fig. 5. The beams without stirrups in A and B Modes failed in shear and collapsed immediately after appearance of the diagonal shear crack, except B3-0 & B3-1 beams where continued to carry further load after the diagonal shear crack appeared until collapse, the inclination angle in the corresponding beams was 14.64°. On the other hand, the RCHBs without stirrups in Mode C continued to carry further load after the diagonal shear crack appeared until the concrete crushed near the loading point. The maximum load capacity and the

Table 3 Test results

Beam code	f_c MPa	E_c GPa	f_t [1] MPa	Load kN			Peak Displacement mm	Effective depth mm	Failure Mode
				First crack	Shear crack	Collapse			
A0-0	44.5	34.2	3.72	45	107	107	1.8	260	S[2]
A0-2	58	34.7	4.2	43	-	215	4.3	--	F[3]
A1-0	60	37	4.4	36	113.5	113.5	2.22	250	S
A2-0	49	35.26	4.04	29	113.2	113.2	2.5	215	S
A2-1	51.5	33.2	4.3	26	115.3	115.3	2.433	215	S
A2-2	59	38.2	4.1	30	-	215	4.53	--	F
A3-0	42.5	34	3.7	29	121	121	2.54	180	S
A3-1	60	37.2	4.15	29	113	113	3.22	180	S
A3-2	59.9	37	4.2	29	-	214	4.82	--	F
B0-0	55	34.1	3.9	42	110	110.3	1.96	260	S
B1-0	53.5	35.2	4.65	39	108.2	108.2	1.9	250	S
B2-0	55.1	50.6	4.26	37	117	117	2.24	215	S
B2-1	53.9	33.2	4.0	36	91	91	2.57	215	S
B3-0	59.5	36.38	4.36	36	109	132	4.64	180	S
B3-1	51.5	35	3.6	33	111.2	123	4.57	180	S
B3-2	59	40.2	4.45	35	-	208	5.97	--	F
C0-0	60.7	34.2	3.87	21	94.4	94.4	2.62	210	S
C1-0	58.5	37.26	4.01	20	77.8	108	5.55	243	S
C2-0	44	33.1	3.69	18	66	101	5.74	265	S
C2-1	61	37	4.3	17	78.6	91.7	6.53	265	S
C2-2	65	39	4.1	26	-	175	5.4	--	F
C3-0	62	37.4	4.35	18	74.3	104	5.33	265	S
C3-1	50.1	32.74	4.3	18	67.2	95.5	5	265	S
C3-2	59	40	3.7	23	-	165	5.5	--	F

[1] Splitting tensile strength; [2] Shear failure Mode;[3] Flexural failure Mode

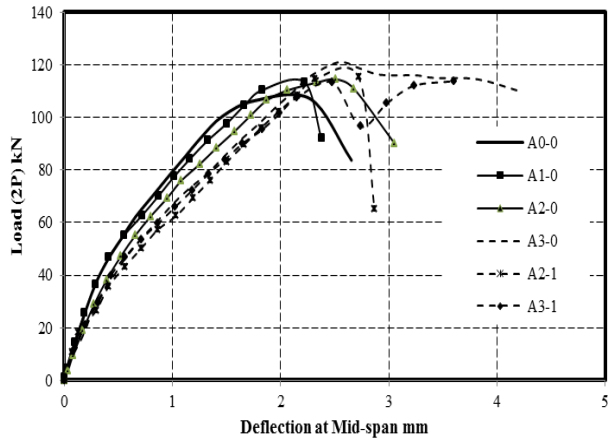

Fig. 6 Load-deflection relationship of beams for Mode A

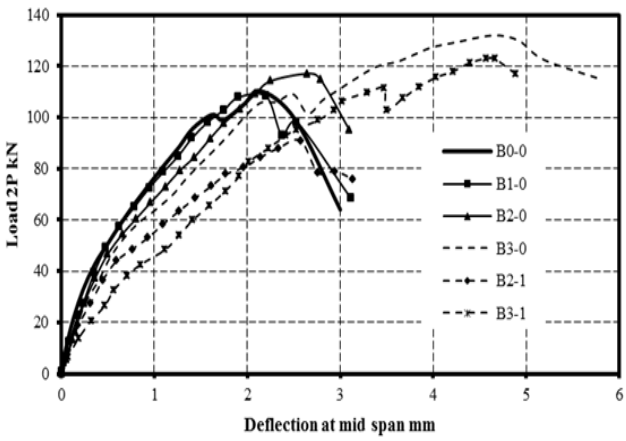

Fig. 7 Load-deflection relationship of beams for Mode B

failure modes for the tested specimens are presented in Table 3.

From the results, it can be observed that the shear capacity of the beams in Mode C decreases with the inclination angle, the negative contribution of the inclination angle due to the vertical component of the axial tensile stress of the flexural reinforcement. However, the positive component for both of the vertical component of the steel stresses in the beams of Mode B and compression chord in Mode A affect positively on the shear strength. It is also inferred from the results of Mode A and B beams that increase of the inclination angle increases the load capacity of the beams due to increasing the vertical component of steel stresses.

3.2 Load-deflection relationship

The values of deflection were measured and recorded using linear variable displacement transducers (LVDTs). CPD type transducers from TML Company were used to measure the displacement and NI cDAQ-9184 data acquisition tool from National Instrument Company was used as data logger. The load-deflection relationships of all beams without stirrup for each mode (A, B and C) are shown in Figs. 6-8.

It can be observed from the figures that load capacities of the beams increase as inclination angle value rises. However, it is important to note that the stiffness of the beams comes down with increase in the inclination angle

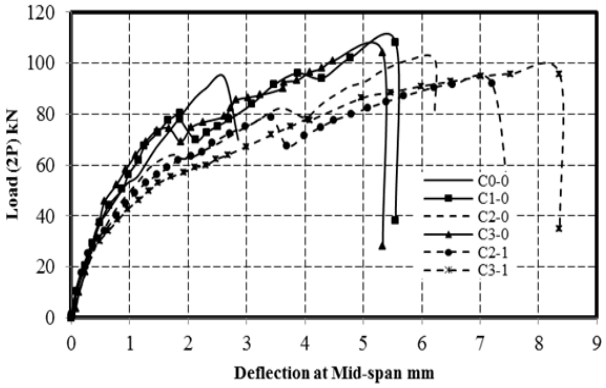

Fig. 8 Load-deflection relationship of beams for Mode C

due to reduction of moment on inertia for the section at inclined segments. The deflection capability of the beams in Modes B and C are higher as compared to the capability of beams of Mode A. This means that the effect of inclined main reinforcement is more apparent than the straight main reinforcement.

3.3 Crack patterns

In general, the failure mode of the RCHBs in shear depends on the pattern of the diagonal shear cracks. During loading process, several crack patterns formed in RCHBs before collapse. Although, the crack propagation and mode of failure have been widely investigated by several experimental and theoretical studies for the prismatic beams, there is very limited research in this topic for RCHBs.

The beams in this study were designed to fail in shear or in flexure. Eighteen beams were designed without shear reinforcement to study the mechanism of the shear failure, and six beams were designed with shear reinforcement to study the flexural failure of RCHBs. In general, all of the beams without stirrups collapsed in shear when diagonal shear cracks appeared suddenly, whereas the beams with shear stirrups failed in flexure or concrete crushing.

At early stage of loading, the flexure cracks appeared along the beam where the first cracks initiated randomly close to the mid-span or below of the loading point. The trajectory of the cracks distribution varied for each beam. Generally, the first cracks were perpendicular to the longitudinal main reinforcements. At higher load, the cracks were inclined and extended toward the position of the loading points. An important observation for the flexure and flexure-shear cracks was that they existed symmetrically on both halves of the beam until collapse. When the diagonal shear crack appeared, all of other cracks stopped growing and some of them were closed. The patterns and the positions of the diagonal shear cracks in beams that collapsed due to diagonal shear crack are presented in Fig. 9. As shown in Fig. 9, the angle of the crack is nearly 45° with the longitudinal flexural reinforcement for Mode A and Mode B, and the angle does not show a definite trend in Mode C.

3.4 Critical effective depth of shear

The RCHBs have variable depth and most of the design codes do not consider the effective depth of RCHBs. The shear effective depth of a RCHB depends on the position of the major diagonal shear crack. Since, the depth is variable; cross-sections are also variable along RCHBs. Therefore, determination of effective depth to be used in shear capacity calculations is confusing. Critical section concept is a powerful and effective solution for this problem. Position of major diagonal shear crack determines the location of the critical section whose depth is called critical effective depth. Based on experimental results, three different modes of failure were observed regarding to the diagonal shear crack as shown in Fig. 10.

The shear cracks in Modes A and B forms 45° with the flexural reinforcement, the position of the critical section for modes A and B are seen to be rather similar and it is certain that the effective depth of the critical section is greater than the support depth. Therefore, the slope signs in Modes A and B are taken as positive. In Mode C, the slope of the critical section was unsteady and so the effective depth was recorded for each beam separately. Therefore, Eq. (1) proposed to predict the effective depth of RCHBs depending on experimental results using regression analysis. The range of the inclination angle is limited between −14.62o and +14.62o to apply the equation.

$$d_c = d_s \cdot F \tag{1}$$

$$\text{Where;} \quad F = \left(1 - 3.04 \tan\alpha\right)^{-0.608} \leq 1.55$$

Where, *dc* is the shear effective depth of the critical section, *ds* is the effective depth of the support and α is the inclination angle.

3.5 Analysis of shear capacity for RCHBs

Although RCHBs are widely used in reinforced concrete structures, most design codes do not offer any instructions for design of the beams. The sections 22.5.1.9 and R22.5.1.9 of ACI 318-14 (2014) confirm to consider the effect of inclined flexural compression in calculating the shear strength of concrete where the internal shear at any section is increased or decreased by the vertical component of inclined flexural stresses. The section 27.4.5.3 of ACI 318-14 (2014) discusses the inclined shear crack in the variable depth beams and recommends measuring the depth at the mid-length of the crack. This part analyses of shear capacity for the tested RCHBs which failed in shear, the experimental strength compared with the estimated strength according to ACI, a sophisticated model called Simplified Modified Compression Field theory and an empirical formula propose by Gulsan *et al.* (2018).

The influence of positive and negative contribution of the inclined flexural reinforcement and the positive contribution of compression chord added to the shear formula of ACI code (Eq. (2)) in term of VCC. The contribution of VCC is positive in Modes (A&B) and negative in Mode C.

$$V = V_C + V_{CC} \tag{2}$$

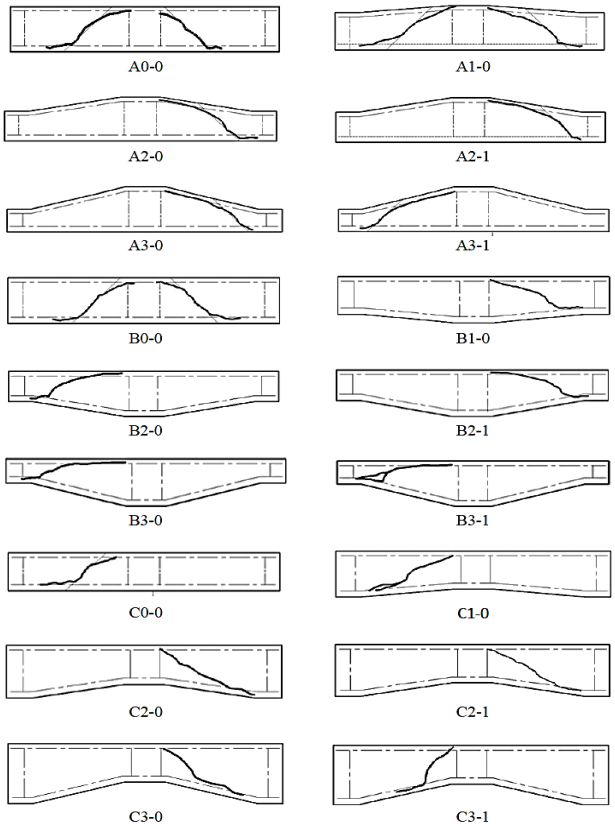

Fig. 9 Diagonal shear cracks

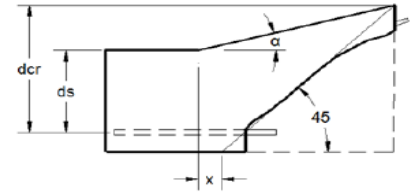

(a) Mode A

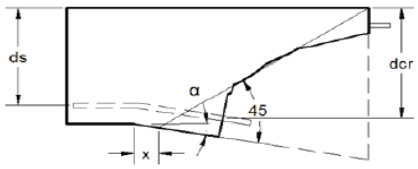

(b) Mode B

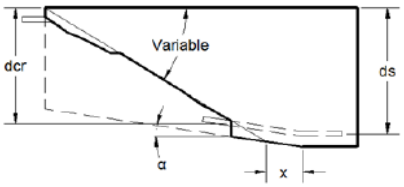

(c) Mode C

Fig. 10 Failure modes for RCHBs

Where; $V_C = 0.17\sqrt{f'_c}\cdot b\cdot d$, $V_{CC} = \frac{M}{Z}.\tan(\alpha)$

Where, M is bending moment at analyzed section, (z≈0.9d) is the arm between the compression and tension forces in the section, and α is inclination angle.

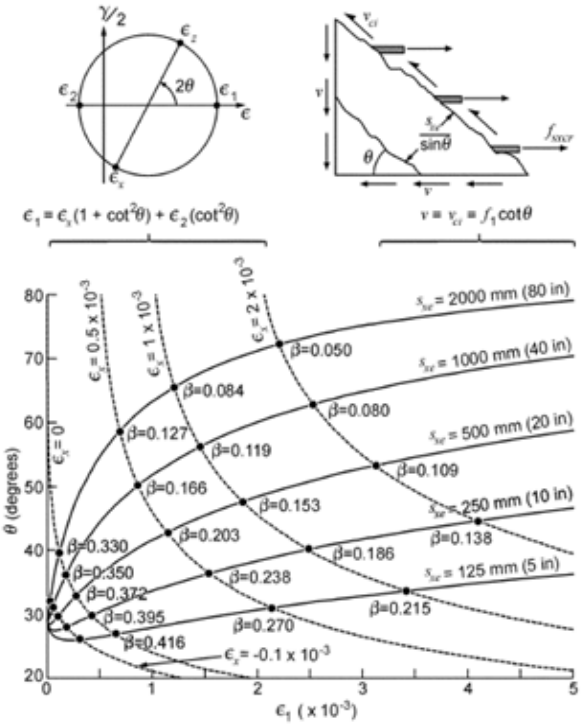

Fig. 11 Values of β and θ for elements without transverse reinforcement (Bentz *et al.* 2006)

Bentz *et al.* (2006), modified a sophisticated model called Simplified Modified Compression Field theory to predict the shear strength by considering the sum of the forces in the *z*-direction for the body diagram shown in Fig. 11, the equation can be arranged to give.

$$v = v_c + v_s = \beta\sqrt{f_c'} + \rho_z f_y \cot\theta \tag{3}$$

Where;

$$\beta = \frac{0.4}{1+1500\cdot\varepsilon_x}\cdot\frac{1300}{1000+S_{xe}}$$

$$\theta = (29\deg + 7000\cdot\varepsilon_x)\left(0.88+\frac{S_{xe}}{2500}\right) \le 75\deg$$

$$S_{xe} = \frac{35\cdot S_x}{a_g+16}$$

Where, v is shear strength of the element, v_c is the concrete contribution, v_s is the transverse reinforcement contribution, β is constant value, f_c' is the compressive strength of concrete, ρ_z is transverse reinforcement ratio, f_y is the yield strength of transverse reinforcement, ε_x is longitudinal strain in compression strut, S_x is spacing between the stirrups and a_g is the aggregate maximum aggregate size.

Eq. (4) which proposed by the authors on the theoretical part (Gulsan *et al*. 2018), the proposed model modified the shear load capacity equation of prismatic beams which adopted by ACI Code for RCHBs by introduction of critical effective depth concept.

$$V = V_C + V_v + V_F + V_N \tag{1}$$

Table 4 Shear strength analysis results

Beam	$V_{test.}$ kN	ACI				MCFT		Eq. (4)	
		V_C kN	V_{CC} kN	V kN	bias	V kN	bias	V kN	bias
A0-0	53.5	44.23	0.00	44.23	0.83	45.86	0.86	51.88	0.97
A1-0	56.75	51.36	5.47	56.83	1.00	56.67	1.00	59.25	1.04
A2-0	56.6	46.41	10.99	57.40	1.01	50.79	0.90	55.49	0.98
A2-1	57.65	47.58	11.20	58.78	1.02	51.99	0.90	56.96	0.99
A3-0	60.5	43.22	17.85	61.07	1.01	48.88	0.81	51.71	0.85
A3-1	56.5	51.36	16.67	68.03	1.20	53.54	0.95	58.15	1.03
B0-0	55.15	49.17	0.00	49.17	0.91	50.98	0.92	56.53	1.04
B1-0	54.1	48.49	5.21	53.71	0.99	53.56	0.99	52.07	0.96
B2-0	58.5	49.21	11.36	60.58	1.04	53.56	0.92	51.66	0.88
B2-1	45.5	48.68	8.84	57.51	1.26	50.57	1.11	51.21	1.13
B3-0	54.5	51.14	16.08	67.22	1.23	52.79	0.97	52.06	0.96
B3-1	55.6	47.58	16.41	63.99	1.15	50.56	0.91	49.59	0.89
C0-0	47.2	41.72	0.00	41.72	0.88	43.26	0.92	49.52	1.05
C1-0	38.9	41.82	-3.75	38.07	0.98	45.39	1.17	42.96	1.10
C2-0	33	35.52	-6.41	29.11	0.88	40.07	1.21	33.86	1.03
C2-1	39.3	41.82	-7.63	34.19	0.87	47.09	1.20	41.82	1.06
C3-0	37.15	42.17	-10.96	31.20	0.84	44.21	1.19	36.55	0.98
C3-1	33.6	37.90	-9.91	27.99	0.83	39.68	1.18	31.18	0.93
Mean					0.99		1.005		0.99
CoV					0.13		0.13		0.07
R^2					0.79		0.67		0.83

Where;

$$V_C = (0.16\sqrt{f_c} + 17\rho_c \frac{V_u d_c}{M_u})bd_c$$

$$V_v = \rho_v f_y bd_c$$

$$V_N = \frac{f_c}{20}\left(2bd_c \frac{30}{f_c} + A_{s''}\left(\frac{E_s}{E_c} - 1\right)\right) \cdot \tan\alpha$$

$$V_F = 0.2A_s f_y \sin\alpha$$

Where; V is the ultimate nominal shear strength, V_C is the contribution of the concrete, V_v is the contribution of the shear reinforcement, V_N is the contribution of the inclined compression chord in Mode C, V_F is the contribution of the inclined flexural reinforcement in Modes (A&B), ρ_c is the reinforcement ratio at the critical section, V_u is shear force and M_u is moment at analyzed section, ρ_v is the transverse reinforcement ratio, f_y is yield strength of the steel, $A_{s''}$ is the compression reinforcement area in Mode A, E_s is elastic modulus of steel, E_c is elastic modulus of concrete and α is the inclination angle. The critical section is predicted in Eq. (1).

Table 4, represents the shear strength analysis results. Shear load capacity values of the RCHBs which are tested in current study calculated according to the Eqs. (2), (3) and (4). The correlations of the results are represented by the mean bias of predicted strength to experimental result, the variance of the bias by coefficient of variation (COV) and R^2 value. The average value of bias found approximately equal to 1.0 for all the models but the variance of the results for Eqs. (2), (3) and (4) which represented by the COV is (0.13, 0.13 & 0.07), respectively. Whereas, R^2 is (0.79, 0.67 & 0.83), respectively. The statistical parameters stated above proved good performance for Eq. (4) in all modes of RCHBs. whereas, ACI code and modified compression field theory did not show a steady response in mode C with increasing of inclination angle.

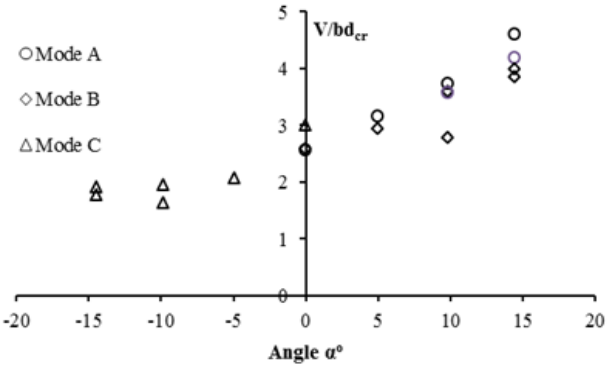

Fig. 12 Influence of the inclination angle on shear strength

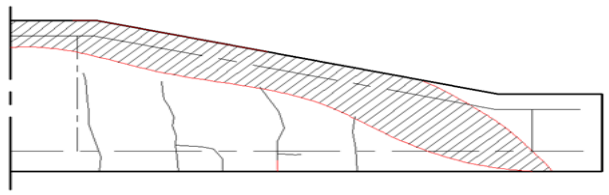

Fig. 13 The compression chord in Mode A

In general, when the load capacity results of the beams belonging to mode A are examined, it can be observed that there is a positive contribution of compression chord which is also stated in the study carried out by Zanuy *et al*. (2015). There is also positive contribution of the positive inclination of the tension chord (Mode B) to the shear strength of RCHBs. This result can be explained by kinking effect of steel longitudinal reinforcement which is proposed by Paulay *et al*. (1974) Kinking effect is related with dowel action of steel reinforcement. According to kinking effect, if there is a noticeable shift between the two main bar axes, the shear capacity contribution of the reinforcement is, where as is cross-sectional area of the longitudinal reinforcement and a is inclination of the reinforcement, which is almost equal to inclination angle of the RCHB. While, inclination of the chord to the support (Mode C) produces negative influence on the capacity of RCHBs.

3.6 Influence of the inclination angle

Influence of the inclination angle on the shear strength capacity of beams is shown in Fig. 12. The inclination angle induces relatively positive effects on the shear strength capacity of RCHBs in Modes A & B. However, the angle has reverse effect on the capacity of beams of Mode C. This matter does not taken into consideration in most building design codes. The interpretation of this situation can be explained as follows:

- In mode A, the zone of the compression chord increases with the inclination angle value as shown in Fig. 13, the compression chord is devoid of the cracks and remains same after the diagonal shear crack appears.

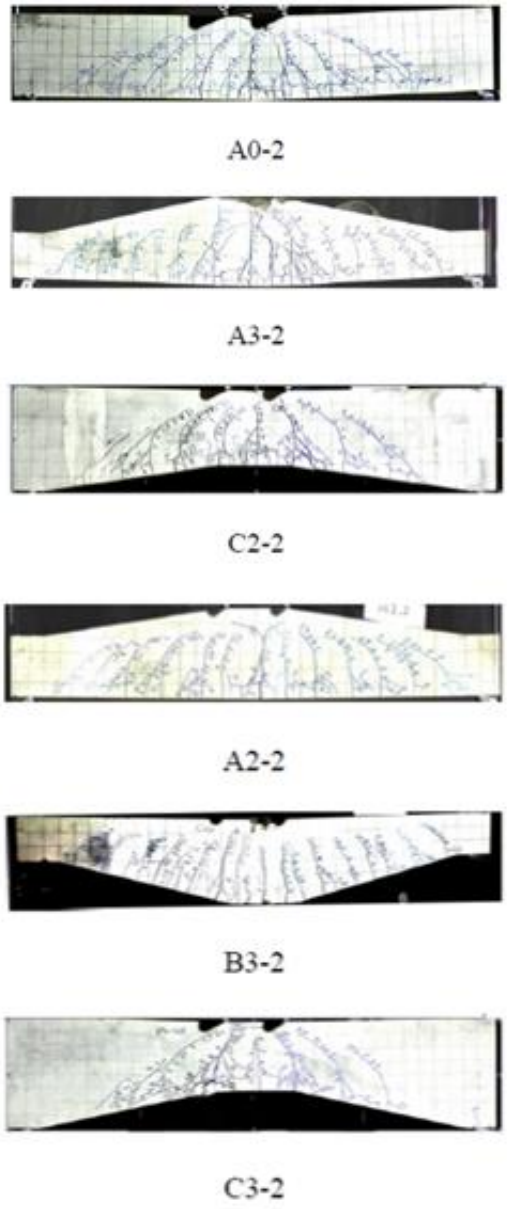

Fig. 14 Flexure failure

• In Mode B, the vertical component of the tensile stress on the longitudinal main reinforcement causes positive effect on the shear capacity of the beams due to its direction. However, the vertical component of the stress in the reinforcement for beams of Mode C exists in reverse direction that leads to a negative effect on the shear strength capacity.

3.7 Influence of the inclined reinforcement

In Mode A, when the capacity of A2-0 and A3-0 beams (reinforcement area is 100 mm^2 in compression zone) were compared with A2-1 and A3-1 beams whose properties are same with A2-0 and A3-0, respectively except reinforcement area in compression zone (308 mm^2), it was concluded that inclined reinforcement in the compression zone had slight effect on the capacity of beams. In Modes B and C, the shear strength capacity was significantly affected

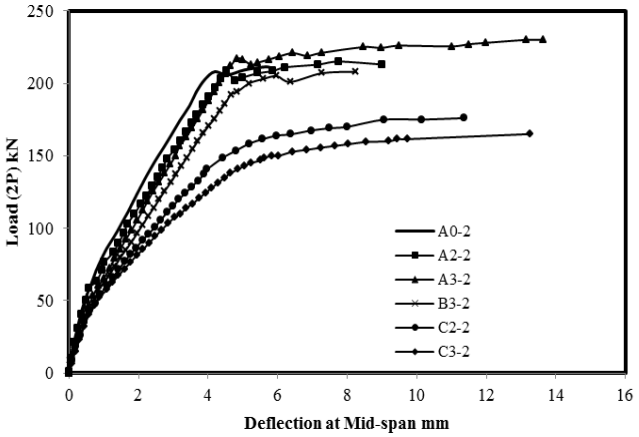

Fig. 15 Load- deflection relationships of beams fail in flexure

by the area of the inclined longitudinal reinforcement in the flexure zone due to the vertical component of the stresses and the truss action of the inclined steel bars.

In Mode B, two steel reinforcement ratios were used where the beams B2-0 & B3-0 were reinforced by 603 mm^2 and the beams B2-1 & B3-1 were reinforced by 402 mm^2. The shear failure load of the beams B2-0 & B2-1 were found to be 117 &91 kN, respectively. The variance in load is 22 % due to variation of area of steel and 7% between the beams B3-0 and B3-1. The similar situation exists for beams of Mode C. For instance, the difference of the failure load is found to be 9% between the beams C2-0 and C2-1 and 8% between the beams C3-0 and C3-1.

3.8 Flexural failure

Six beams out of twenty four beams were reinforced with shear stirrups (ϕ 8 mm at each 100 mm). The beam (A0-2) has a prismatic section and the other beams (A2-2, A3-2, B3-2, C2-2 & C3-2) are RCHBs. The load-deflection curves and crack patterns of these beams are shown in Fig. 14 and Fig. 15, respectively. The type of the failure for all of these beams was flexure and concrete crushing as shown in Fig. 14. While the reinforcement yielded at mid-span of beams for Mode A, the position of yielding shifted to near of inclination point for beams of Modes B&C. After yielding, the load remained constant and the deflection increased. After a while the load increased about 5-10 % of the yield load till the concrete crushing.

The results does not show a significant difference in the value of the maximum load between the prismatic beam and the A series beams of A0-2, A2-2 & A3-2; the results are 215 kN, 215 kN and 214 kN, respectively. The explanation is the flexural crack which led to failure is near of the prismatic zone and the effective depth of the flexure is the same of the prismatic beam.

However, as seen from the load-deflection curves (Fig. 15), the stiffness of RCHBs is smaller as compared to prismatic beam due to variable depth along the RCHBs. The beams of Mode C, C2-2 and C3-2 also failed in flexure or concrete crushing at load 175 and 165 kN, respectively. According to the results, it can be generally said that there

is no a significant difference in the load capacity between beams of Modes A and B and prismatic beam. However, the stiffness of Mode A and B beams decreases slightly. Lastly, the capacity and stiffness decreases apparently when the beams of Mode C are preferred. In general, the reduction of concrete volume in RCHBs did not reduce the efficiency of the beam in flexural behavior.

3.9 Inspection of crack propagation

Reinforced concrete members have a complex crack pattern depending on the geometry of the member and material properties. The crack patterns that occur in RCHBs can differ from ones that exist in prismatic beams. Moreover, the form of cracks can exhibit variety between modes of the RCHBs. The inspection of the crack propagation for all of the tested beams is presented in the Appendix part of the article. In general, the initial cracks appear as perpendicular to the flexural reinforcement in low load levels and develop at higher loads. The distinctive points observed from the tests for crack propagation in the beams can be listed as follows; 1) The ends of the flexural cracks extend into the upper edge of the beam as parallel at high loads for the beams of Mode A and Mode B. 2) Splitting cracks occur along the reinforcement bar in beams of Mode C, these cracks are result of the take-off force that occurs from the reinforcement to the concrete cover. 3) The crack propagation in the beams that fail in flexure mode is similar for all of them. 4) In C series the concrete cover on the bending point of the reinforcement took off due to the concentration of the stresses in the bending point, the reason is the negative component of the tensile stress in reinforcement bars.

4. Conclusions

This study investigated the mechanical behavior of different modes of Reinforced Concrete Haunched Beams (RCHBs). An experimental program consisting of 24 beams was implemented. The RCHBs were classified into three modes namely as, A, B and C according to the inclination shape. The parameters that considered in this study were the inclination angle, the ratio of inclined reinforcement, shear reinforcement and the geometry of the beam. Moreover, cracks propagation was observed for each beam separately. As a result of the study, the following conclusions can be drawn:

- In general, two failure modes were observed as a result of the loading tests, i.e., the beams without shear stirrups fail due to diagonal shear, whereas flexure-concrete crushing failure are observed in the beams that contain shear stirrups.
- In the beams of Mode A and B, vertical component of the stress that occurs in reinforcement contributes to the load capacity of them and so increases the capacity. However, beams of mode C shows contrary behavior and the capacity of them are lower due to the negative contribution of inclination angle to the shear strength. Therefore the inclination angle is assumed to be positive for beams of modes A and B, while negative for beams of Mode C. Although, the effective depths the beams of Mode C are higher, the shear strengths of them are lower.
- For all considered RCHB Mode (A, B and C), stiffness of the beams decreases slightly, as the inclination angle increases.
- For all beams, the first crack is pure flexure crack that appears in the middle of them. The flexure cracks form perpendicular to the flexure reinforcement bars regardless of the beam type. Flexural cracks continue to propagate up to 50-60% of the ultimate load. At higher load ranges, most of the cracks, except ones close to the middle of the beams, turn to be inclined shear-flexure cracks. Furthermore, for the beams without shear reinforcement, propagation of the cracks in inclined direction continues to upper edge of the beams until one of the cracks suddenly expands to form the critical diagonal shear crack that stops the formation and propagation of other cracks and finally causes the failure.
- Since the depth changes continuously in RCHBs, determination of the critical section is very crucial for correct prediction of the mechanical behavior of them. Therefore, Eq. (1) proposed to predict the shear effective depth for all modes of RCHBs by taking inspection of crack propagation into account.
- From the results, can be concluded that mechanical behavior of RCHBs that exhibit flexural behavior is similar to the behavior of prismatic beams, except beams of Mode C. Due to the inclination of beams with negative angle, load capacities are lower and splitting cracks appear in tension side for beams of Mode C.
- The post-peak behaviors of the beams differ from each other. In prismatic beams and RCHBs of Modes A and B, the load value tends to decrease after the critical crack forms, except B3-0 & B3-1 beams which have inclination angle of 14.62o. However, the load continues to increase until the collapse of beams due to the concrete fracture at loading point for beams of Mode C.
- Although RCHBs contain lower concrete volume as compared to prismatic beams, shear strength capacity increases in RCHBs and the flexural efficiency, crack patterns and failure modes are not affected negatively. Therefore, preference of reinforced concrete haunched beams is more economical provided that geometry of them is suitable for the constructions and structures.

References

Albegmprli, H.M. (2017), "Experimental investigation and stochastic FE modeling of reinforced concrete haunched beams", PhD Thesis, Gaziantep University, Turkey.

Albegmprli, H.M., Abdulkadir, Ç., Gulsan, M.E. and Kurtoglu, A.E. (2015), "Reliability analysis of reinforced concrete haunched beams shear capacity based on stochastic nonlinear FE analysis", *Comput. Concrete*, **15**, 259-277.

Archundia-Aranda, H.I., Tena-Colunga, A. and Grande-Vega, A. (2013), "Behavior of reinforced concrete haunched beams subjected to cyclic shear loading", *Eng. Struct.*, **49**, 27-42.

Bentz, E.C., Vecchio, F.J. and Collins, M.P. (2016), "Simplified modified compression field theory for calculating shear strength of reinforced concrete elements", *Struct. J.*, **103**, 614-624.
Chenwei, H. and Matsumoto, K. (2015), "Shear failure mechanism of reinforced concrete Haunched beams", *J. JSCE*, **3**, 230-245.
Debaiky, S.Y. and Elniema, E.I. (1982), "Behavior and strength of reinforced concrete haunched beams in shear", *ACI Struct. J.*, **79**, 184-194.
DIN 1045-01 (2001), Tragwerke aus Beton, Stahlbeton und Spannbeton, Teil 1Bemessungund Konstruktion, Beuth Verlag GmbH, Berlin, Germany.
El-Niema, E.I. (1988), "Investigation of concrete haunched t-beams under shear", *J. Struct. Eng.*, ASCE, **114**, 917-930.
Gulsan, M.E., Albegmprli, H.M. and Cevik, A. (2018), "Finite element and design code assessment of reinforced concrete haunched beams", *Struct. Eng. Mech.*, **66**, 423-438.
MacLeod, I.A. and Houmsi, A, (1994), "Shear strength of haunched beams without shear reinforcement", *ACI Struct. J.*, **91**, 79-89.
Naik, P.K. and Manjunath, M. (2017), "Pushover analysis of multi-storey frame structure with haunched beam", *Int. J. Trend Res. Develop.*, **4**(3), 333-336.
Nghiep, V.H. (2011), "Shear design of straight and haunched concrete beams without stirrups", Dissertation, Technischen Universität Hamburg, Germany.
Paulay, T., Park, R. and Phillips, M.H. (1974), "Horizontal construction joints in cast-in-place reinforced concrete", *Spec. Pub.*, **42**, 599-616.
Stefanou, G.D. (1983), "Shear resistance of reinforced concrete beams with non-prismatic sections", *Eng. Fract. Mech.*, **18**, 643-666.
Tena-Colunga, A., Hans, I.A. and Oscar, M.G. (2008), "Behavior of reinforced concrete haunched beams subjected to static shear loading", *Eng. Struct.*, **30**, 478-492.
Zanuy, C., Juan, M.G. and Luis, A. (2015), "Fatigue behavior of reinforced concrete Haunched beams without stirrups", *ACI Struct. J.*, **12**, 371-382.

CC

Appendix: Cracks propagation

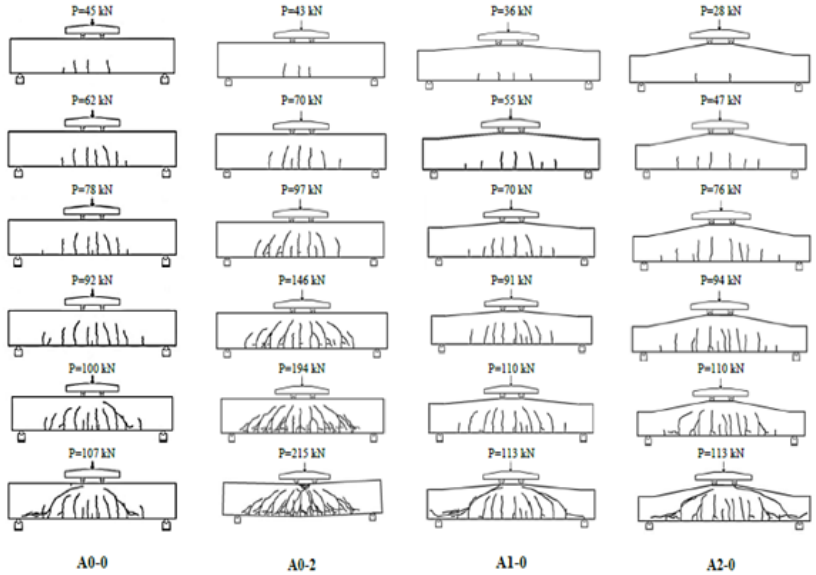

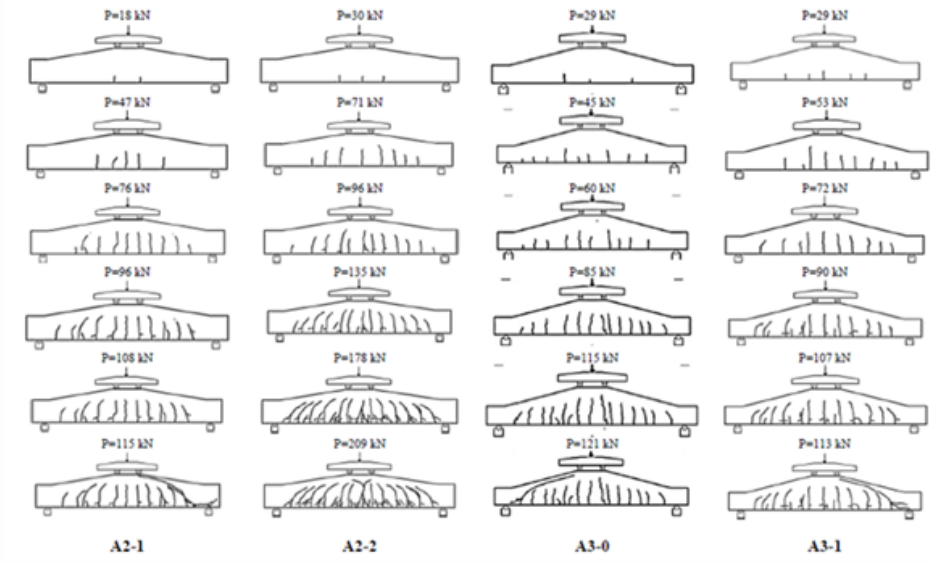

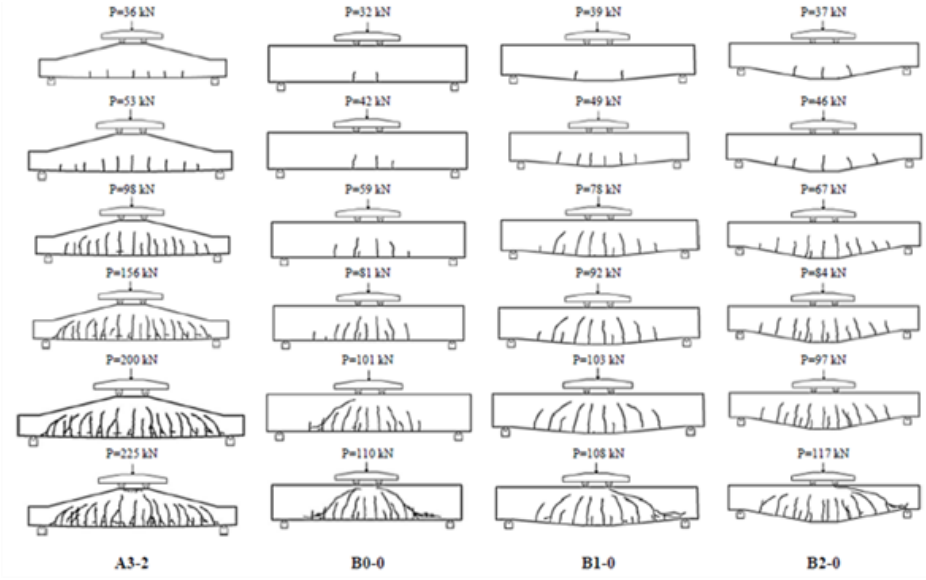

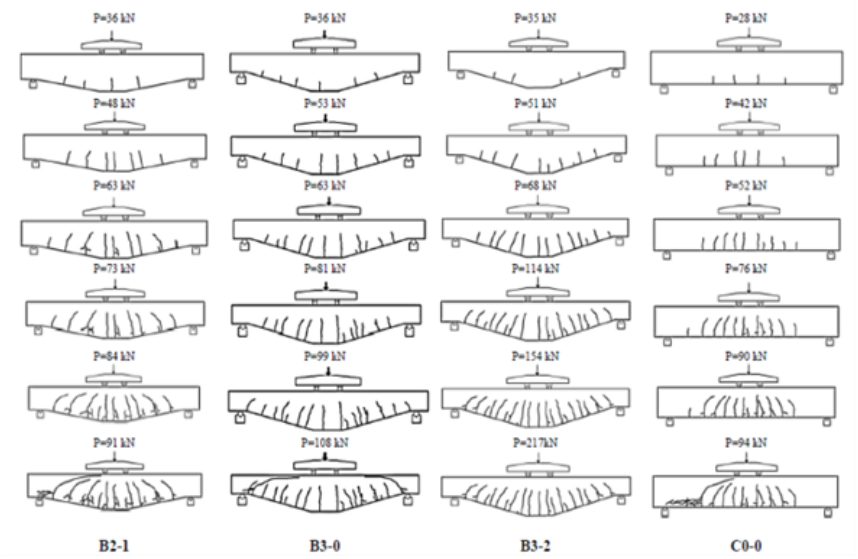
P=36 kN
P=48 kN
P=63 kN
P=73 kN
P=84 kN
P=91 kN
B2-1
P=36 kN
P=53 kN
P=63 kN
P=81 kN
P=99 kN
P=108 kN
B3-0
P=35 kN
P=51 kN
P=68 kN
P=114 kN
P=154 kN
P=217kN
B3-2
P=28 kN
P=42 kN
P=52 kN
P=76 kN
P=90 kN
P=94 kN
C0-0

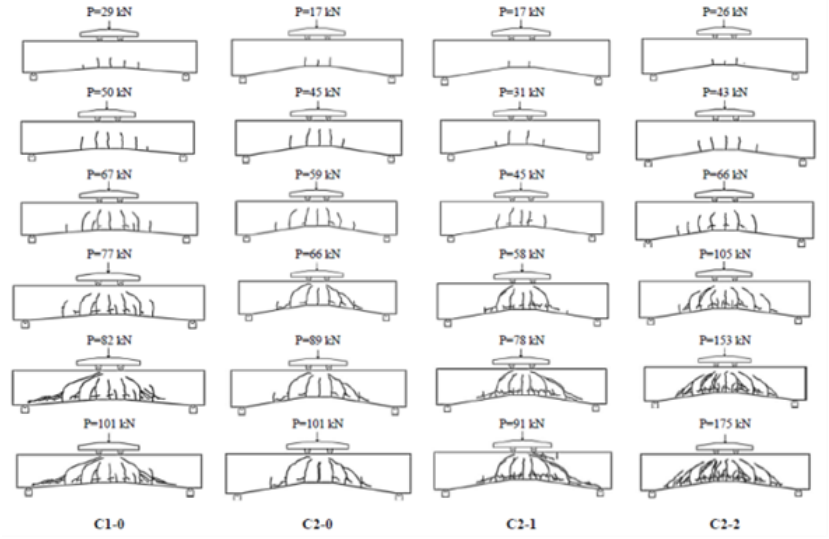
P=29 kN
P=50 kN
P=67 kN
P=77 kN
P=82 kN
P=101 kN
C1-0
P=17 kN
P=45 kN
P=59 kN
P=66 kN
P=89 kN
P=101 kN
C2-0
P=17 kN
P=31 kN
P=45 kN
P=58 kN
P=78 kN
P=91 kN
C2-1
P=26 kN
P=43 kN
P=66 kN
P=105 kN
P=153 kN
P=175 kN
C2-2

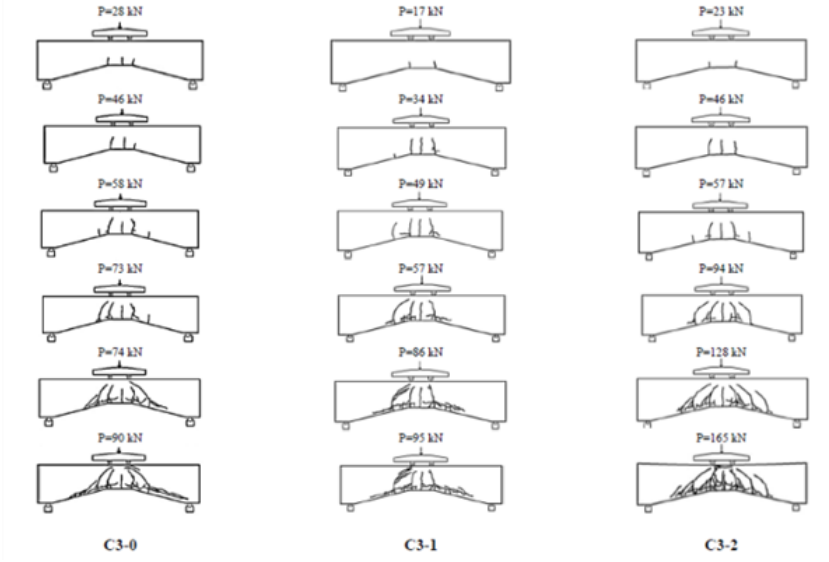
P=28 kN
P=46 kN
P=58 kN
P=73 kN
P=74 kN
P=90 kN
C3-0
P=17 kN
P=34 kN
P=49 kN
P=57 kN
P=86 kN
P=95 kN
C3-1
P=23 kN
P=46 kN
P=57 kN
P=94 kN
P=128 kN
P=165 kN
C3-2